

---

# DEFENDING AGAINST ADVERSARIAL ATTACKS BY SUPPRESSING THE LARGEST EIGENVALUE OF FISHER INFORMATION MATRIX

---

**Chaomin Shen**

School of Computer Science and Technology  
East China Normal University  
Shanghai, China  
cmshen@cs.ecnu.edu.cn

**Yaxin Peng**

Department of Mathematics  
Shanghai University  
Shanghai, China  
yaxin.peng@shu.edu.cn

**Guixu Zhang**

School of Computer Science and Technology  
East China Normal University  
Shanghai, China  
gxzhang@cs.ecnu.edu.cn

**Jinsong Fan\***

College of Mathematics and Physics  
Wenzhou University  
Wenzhou, Zhejiang, China  
fjs@wzu.edu.cn

## ABSTRACT

We propose a scheme for defending against adversarial attacks by suppressing the largest eigenvalue of the Fisher information matrix (FIM). Our starting point is one explanation on the rationale of adversarial examples. Based on the idea of the difference between a benign sample and its adversarial example is measured by the Euclidean norm, while the difference between their classification probability densities at the last (softmax) layer of the network could be measured by the Kullback-Leibler (KL) divergence, the explanation shows that the output difference is a quadratic form of the input difference. If the eigenvalue of this quadratic form (a.k.a. FIM) is large, the output difference becomes large even when the input difference is small, which explains the adversarial phenomenon. This makes the adversarial defense possible by controlling the eigenvalues of the FIM. Our solution is adding one term representing the trace of the FIM to the loss function of the original network, as the largest eigenvalue is bounded by the trace. Our defensive scheme is verified by experiments using a variety of common attacking methods on typical deep neural networks, e.g. LeNet, VGG and ResNet, with datasets MNIST, CIFAR-10, and German Traffic Sign Recognition Benchmark (GTSRB). Our new network, after adopting the novel loss function and retraining, has an effective and robust defensive capability, as it decreases the fooling ratio of the generated adversarial examples, and remains the classification accuracy of the original network.

**Keywords** Adversarial attack · Adversarial defense · Fisher information matrix · Loss function · Deep neural network

## 1 Introduction

Adversarial examples are samples added with carefully designed perturbations, such that those perturbed samples will be misclassified by the Deep Neural Networks (DNNs) for classification [1, 2]. In certain critical circumstances, such as autonomous driving or security sensitive tasks, it is crucial to avoid such adversarial phenomenon. Therefore, defending against adversarial attacks becomes a hot topic in machine learning [3].

In order to avoid/alleviate the adversarial phenomenon, it is important to reveal the rationale of adversarial examples. Many explanations have been provided, yet no consensus has been reached. For example, [1] suggested that the adversarial phenomenon is due to the excessive non-linearity of the neural networks. Later the idea was modified by

---

\*Corresponding author

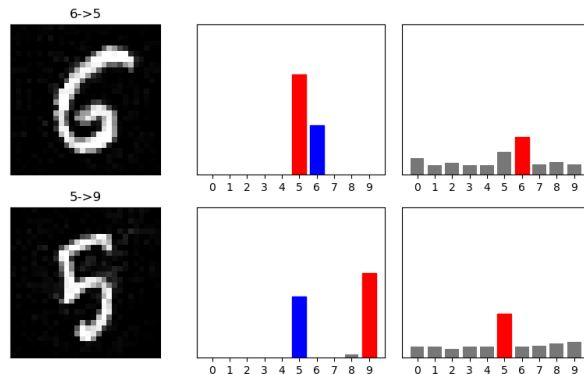


Figure 1: Visualization for the results of our defensive scheme. Left column: two adversarial examples generated on MNIST via the attack method OSSA. Middle column: the predicted label distributions by the original DNN, i.e., result without using our defensive scheme. The blue/red bar represents the true/misclassified label, respectively. In row 1, '6' is misclassified as '5', and in row 2, '5' is misclassified as '9'. Right column: the predicted label distribution of our scheme by modifying the loss function of the original DNN. This figure demonstrates that we survive under the adversarial attack and obtain the correct result. With our scheme, the label distribution is smoothed but the correct label has the highest probability.

models being too linear [4]. Another explanation claimed that the phenomenon results from the high curvature regions on the decision boundary [5].

In [6], the authors suggested that the vulnerability of DNNs may be caused by the large value of the largest eigenvalue of the Fisher Information Matrix (FIM) induced by the input sample. Their idea is that the input difference of the DNNs between a benign sample and its adversarial example is measured by the Euclidean norm, while the output difference between their classification probability density vectors at the last (softmax) layer could no longer be measured by the Euclidean norm, and should be measured by other suitable "distance" such as the Kullback-Leibler (KL) divergence. Then, the output difference is a quadratic form of the input difference, and the quadratic matrix is the FIM. Thus, the adversarial example can be constructed by setting the perturbation direction as the direction of the eigenvector for the largest eigenvalue. This method is called One Step Spectral Attack (OSSA).

Inspired by [6], in this paper we propose a method for defending against adversarial attacks by only modifying the loss function of the original DNN so that the largest eigenvalue of the FIM is suppressed. Here we first illustrate our result in Figure 1. Details will be given in Section 3.

The novelties of the paper lie in:

- 1) Our scheme is simple yet effective, as it only adds one regularization term to the loss function of original DNNs and needs to retrain only once. With our scheme, the capability of defending against adversarial examples can be significantly improved;
- 2) Our scheme is explainable, as it is based on mathematical deduction. After the softmax layer, its output probability distribution is similar to that of label smoothing [7], while ours provides a reasonable explanation.

The rest of the paper is organized as follows. Section 2 reviews some related work on adversarial attacks and defense. Section 3 describes our defensive scheme in detail with mathematical deduction, and makes a comparison with label smoothing. Section 4 shows the experiments on defending against various white-box and black-box attacks on a variety of datasets and DNNs. The paper is concluded in Section 5.

## 2 Related Work

In this section, we review some related work on adversarial attacks and defense.

### Adversarial attacks

Adversarial attacks can be classified based on different criteria, while the most important and common criterion is according to the measure of the perturbation, i.e., they can be classified as  $l_0$ ,  $l_2$  and  $l_\infty$  attacks. Adversarial attacks can also be targeted or non-targeted according to the misclassified label concerned, one-step attack or multi-step attack

according to whether the adversarial example is generalized by one-step or by iteration, or white-box or black-box attack according to whether the network structure and corresponding weights are known.

[4] proposed a simple and fast  $l_\infty$  attack, called the Fast Gradient Sign Method (FGSM), by using the sign of the gradient to generate perturbation. [8, 9] extended the gradient method to  $l_2$  norm, and proposed the Basic Iterative Method (BIM), and other consequent more powerful attacking methods. [10] proposed the Carlini-Wagner (CW) attack, which includes  $l_0, l_2, l_\infty$  norms and can be applied to targeted or non-targeted attacks. [11] developed DeepFool, an  $l_2$ -norm and non-targeted method which uses iteration to push the image to the classification boundary iteratively. Jacobian-based Saliency Map Attack (JSMA), an  $l_0$ -norm targeted method proposed by [12], minimizes the number of modified pixels so that the image is misclassified as a particular (wrong) target class. Those more powerful methods all adopt the iterative optimization methods, such that the perturbation is small yet effective. To achieve such a goal, simple methods, e.g., FGSM, usually need to conduct searches on certain particular perturbation space, such as binary search.

### Adversarial defenses

The adversarial phenomenon naturally spawns many works on defending against adversarial attacks for DNNs. To date, these adversarial defenses can be roughly categorized into the following three types:

- 1) Data pre-processing. This kind of method pre-processes the input data during the training and testing, which includes image gradient processing, transforming, denoising, enhancing, or a small scale network training to pre-process the input.
- 2) Classification model modification. This kind of method increases/deletes/modifies certain layers, or modifies the loss function and the activation function.
- 3) Robust learning. This kind of method includes adversarial training and robust gradient descent techniques. Note that here adversarial training is in its narrow sense, meaning using adversarial examples as a part of the training data.

Adversarial training [1] trains the model by repeatedly feeding the adversarial examples into the training set, such that the new model can possess certain defensive capability. Due to its simplicity and effectiveness, many adversarial attacking methods, e.g., [6], also used adversarial training for evaluation. [6] also proposed a novel approach for adversarial detection, i.e., when an adversarial example is detected, warning is triggered and further processing aborts.

[13] proposed a robust optimization method called Projected Gradient Descent (PGD). Based on the corollary of a classical result in [14], PGD uses the gradient descent method to obtain an optimized defensive network. Note that PGD is also an attack method from another point of view. [13] was adopted by many defensive methods such as the thermometer encoding [15].

More recently, the method of Label Smoothing Regularization (LSR) receives attention in adversarial defense. Introduced by [7], LSR was first used for improving the performance of Inception network and now has become a common technique for DNN regularization. LSR can improve the generalization capability and also increase the classification accuracy by a small amount. The role of LSR in adversarial defense was observed by experiments in [16]. [17] proposed many variants of LSR for adversarial defense.

## 3 Proposed Scheme

In this section, we first summarize the mechanism of adversarial phenomenon proposed in [6]. Then based on that mechanism, we propose our solution for defending against adversarial attacks, followed by the analysis of our scheme.

### 3.1 Our starting point

The starting work of our defensive scheme is [6]. Its basic idea can be summarized as follows.

Given a (gray) image of  $m \times n$ , the aim of a classification problem is to classify it as  $K$  classes.

Suppose that the image has been pulled as a (column) vector  $\mathbf{x}$  with the length  $m \times n$ , and its perturbed image is  $\mathbf{x}' = \mathbf{x} + \boldsymbol{\eta}$ , where  $\boldsymbol{\eta}$  is the perturbation. After certain DNN, their softmax layer outputs are  $\mathbf{s}(\mathbf{x}) = [p_1(\mathbf{x}), \dots, p_K(\mathbf{x})]^T$  and  $\mathbf{s}(\mathbf{x} + \boldsymbol{\eta}) = [p_1(\mathbf{x}'), \dots, p_K(\mathbf{x}')]^T$ , where  $p_i \geq 0$  for  $i = 1, \dots, K$  and  $\sum_{i=1}^K p_i = 1$ .

Denote the probability that  $\mathbf{x}$  belongs to the  $i$ -th class by  $p(\mathbf{y}_i|\mathbf{x})$ , where  $\mathbf{y}_i$  is a one hot vector  $\mathbf{y}_i = [y_1, \dots, y_i, \dots, y_K]^T$  where  $y_i = 1$  and  $y_j = 0$  for  $j \neq i$ . Thus,  $p(\mathbf{y}_i|\mathbf{x}) = p_i(\mathbf{x})$ , and  $\mathbf{s}(\mathbf{x}) = [p(\mathbf{y}_1|\mathbf{x}), \dots, p(\mathbf{y}_K|\mathbf{x})]^T$ . The classification label  $i$  is determined by  $i = \arg \max_j p_j(\mathbf{x})$ .

The distance between  $\mathbf{x}$  and  $\mathbf{x} + \boldsymbol{\eta}$  can be measured by  $l_k$  norm, where  $k$  can be chosen as 1, 2, or  $\infty$ . In [6],  $k$  is chosen as 2, i.e., the Euclidean norm is used. However, the Euclidean norm cannot be used as a measure of distance between  $\mathbf{s}(\mathbf{x})$  and  $\mathbf{s}(\mathbf{x}')$ , as  $\{\mathbf{s}(\mathbf{x})\}$  does not form a linear space. A suitable measure is the Kullback-Leibler (KL) divergence, denoted by  $D_{KL}$ .

Let  $\mathbf{y}$  be the random variable ranging from  $\mathbf{y}_1$  to  $\mathbf{y}_K$  with the distribution density  $p(\mathbf{y}|\mathbf{x})$ , where  $p(\mathbf{y}|\mathbf{x}) = p(\mathbf{y}_i|\mathbf{x}) = p_i(\mathbf{x})$  if  $\mathbf{y} = \mathbf{y}_i$  for  $i = 1, \dots, K$ . Then we can expand  $D_{KL}$  using the 2nd order Taylor expansion, i.e.,

$$D_{KL}(\mathbf{s}(\mathbf{x})\|\mathbf{s}(\mathbf{x} + \boldsymbol{\eta})) = \mathbb{E}_{\mathbf{y}}[\log \frac{p(\mathbf{y}|\mathbf{x})}{p(\mathbf{y}|\mathbf{x} + \boldsymbol{\eta})}] \approx \frac{1}{2} \boldsymbol{\eta}^T \mathbf{G}_{\mathbf{x}} \boldsymbol{\eta}, \quad (1)$$

where  $\mathbf{G}_{\mathbf{x}} = \mathbb{E}_{\mathbf{y}}[(\nabla_{\mathbf{x}} \log p(\mathbf{y}|\mathbf{x}))(\nabla_{\mathbf{x}} \log p(\mathbf{y}|\mathbf{x}))^T]$  is the FIM of  $\mathbf{x}$ .

Note that the quadratic form (1) becomes large if the largest eigenvalue of the FIM,  $\lambda_{\max}(\mathbf{G}_{\mathbf{x}})$ , is large. Therefore, adversarial phenomenon may occur if  $\lambda_{\max}(\mathbf{G}_{\mathbf{x}})$  is large.

The quadratic form (1) can be used to generate the adversarial attack. OSSA is constructed by maximizing (1) under some constraints, i.e.,

$$\max_{\boldsymbol{\eta}} \boldsymbol{\eta}^T \mathbf{G}_{\mathbf{x}} \boldsymbol{\eta} \quad \text{s.t.} \quad \|\boldsymbol{\eta}\|_2^2 = \varepsilon, \quad J(\mathbf{y}, \mathbf{x} + \boldsymbol{\eta}) > J(\mathbf{y}, \mathbf{x}),$$

where  $\varepsilon$  denotes the squared norm of the perturbation, and  $J$  is the loss function.

Therefore, the problem of constructing adversarial examples is converted to the problem of finding the largest eigenvalue  $\lambda_{\max}(\mathbf{G}_{\mathbf{x}})$  and its corresponding eigenvector  $\boldsymbol{\eta}$  of  $\mathbf{G}_{\mathbf{x}}$ , i.e.,  $\mathbf{G}_{\mathbf{x}} \boldsymbol{\eta} = \lambda_{\max} \boldsymbol{\eta}$ . That is, the perturbation  $\boldsymbol{\eta}$  should be the product of the length  $\sqrt{\varepsilon}$  and the normalized eigenvector corresponding to the largest eigenvalue.

### 3.2 Our Scheme

This subsection is devoted to how to construct our defensive scheme for adversarial attacks.

Since larger eigenvalue of  $\mathbf{G}_{\mathbf{x}}$  may cause the larger difference of KL divergence, and consequently cause the adversarial phenomenon, one solution for defending against adversarial attacks is to control  $\lambda_{\max}(\mathbf{G}_{\mathbf{x}})$  induced by the input sample.

A natural approach is to add a regularization term to the loss function of the original network to suppress the largest eigenvalue  $\lambda_{\max}(\mathbf{G}_{\mathbf{x}})$  of the FIM  $\mathbf{G}_{\mathbf{x}}$ , i.e., modify the loss function as

$$L(\Theta) + \mu \cdot \lambda_{\max}(\mathbf{G}_{\mathbf{x}}), \quad (2)$$

where  $\mu$  is the regularization parameter,  $L(\Theta)$  is the loss function of the original network, and  $\Theta$  is the set of parameters of the original network.

Two problems prevent the direct use of the loss function (2). One is that the matrix  $\mathbf{G}_{\mathbf{x}}$  is too large. For example, given a  $1000 \times 1000$  image, it is a vector of length  $10^6$  after conversion, which means that  $\mathbf{G}_{\mathbf{x}}$  is  $10^6 \times 10^6$ . The other is that it is difficult to explicitly write down the formula of  $\lambda_{\max}(\mathbf{G}_{\mathbf{x}})$ , even if we can tackle the big matrix.

The first problem can be settled by the following strategy. We turn our focus from  $\mathbf{G}_{\mathbf{x}}$  to a new matrix  $\mathbf{G}_{\mathbf{s}}$ , where  $\mathbf{s}$  is the output of the softmax layer  $\mathbf{s} = [p_1(\mathbf{x}), \dots, p_K(\mathbf{x})]^T$ . Similar to  $\mathbf{G}_{\mathbf{x}}$ , we have

$$\mathbf{G}_{\mathbf{s}} = \mathbb{E}_{\mathbf{y}}[\nabla_{\mathbf{s}} \log p(\mathbf{y}|\mathbf{s}) \cdot [\nabla_{\mathbf{s}} \log p(\mathbf{y}|\mathbf{s})]^T].$$

Note that  $\mathbf{G}_{\mathbf{s}}$  is a  $K \times K$  positive definite matrix.

We have

$$\begin{aligned} \boldsymbol{\eta}^T \mathbf{G}_{\mathbf{x}} \boldsymbol{\eta} &= \boldsymbol{\eta}^T \mathbb{E}_{\mathbf{y}}[J^T \nabla_{\mathbf{s}} \log p(\mathbf{y}|\mathbf{s}) [J^T \nabla_{\mathbf{s}} \log p(\mathbf{y}|\mathbf{s})]^T] \boldsymbol{\eta} \\ &= \boldsymbol{\eta}^T J^T \mathbb{E}_{\mathbf{y}}[\nabla_{\mathbf{s}} \log p(\mathbf{y}|\mathbf{s}) \cdot [\nabla_{\mathbf{s}} \log p(\mathbf{y}|\mathbf{s})]^T] J \boldsymbol{\eta}, \end{aligned}$$

where  $J = \left( \frac{\partial s^i}{\partial x^\alpha} \right)$  is a  $K \times mn$  Jacobian of  $\mathbf{s} = \mathbf{s}(\mathbf{x})$ , and  $\nabla_{\mathbf{x}} = J^T \nabla_{\mathbf{s}}$ .

Then,

$$\boldsymbol{\eta}^T \mathbf{G}_{\mathbf{x}} \boldsymbol{\eta} = \boldsymbol{\eta}^T J^T \mathbf{G}_{\mathbf{s}} J \boldsymbol{\eta}.$$

Thus the first problem is settled by converting calculating the largest eigenvalue and corresponding eigenvector of a large  $mn \times mn$  matrix into calculating those of a much smaller  $K \times K$  matrix.

Then the loss function can be further written as

$$L(\Theta) + \mu \lambda_{\max}(\mathbf{G}_{\mathbf{s}}). \quad (3)$$

Note that although (2) is greatly simplified as (3), the problem of no explicit expression for  $\lambda_{\max}(G_s)$  still exists.

The second problem could be solved via replacing the largest eigenvalue  $\lambda(G_s)$  by the trace of  $G_s$ , as the trace equals the summation of all eigenvalues which are all positive due to the positive definiteness of  $G_s$ . Thus, our loss function changes to

$$L(\Theta) + \mu \operatorname{tr} G_s.$$

The trace of  $G_s$  can be calculated as follows.

$$\begin{aligned} \operatorname{tr} G_s &= \operatorname{tr} \mathbb{E}_{\mathbf{y}} [\nabla_{\mathbf{s}} \log p(\mathbf{y}|\mathbf{s}) \cdot [\nabla_{\mathbf{s}} \log p(\mathbf{y}|\mathbf{s})]^T] \\ &= \int_{\mathbf{y}} p(\mathbf{y}|\mathbf{s}) [\operatorname{tr} ((\nabla_{\mathbf{s}} \log p(\mathbf{y}|\mathbf{s}))^T (\nabla_{\mathbf{s}} \log p(\mathbf{y}|\mathbf{s})))] \\ &= \int_{\mathbf{y}} p(\mathbf{y}|\mathbf{s}) \cdot \|\nabla_{\mathbf{s}} \log p(\mathbf{y}|\mathbf{s})\|_2^2 \\ &= \sum_{i=1}^K p_i \sum_{j=1}^K (\nabla_{p_j} \log p(\mathbf{y}_i|\mathbf{s}))^2 \\ &= \sum_{i=1}^K p_i \sum_{j=1}^K (\nabla_{p_j} \log p_i)^2 \\ &= \sum_{i=1}^K \frac{1}{p_i}. \end{aligned}$$

Thus the final loss function for the defensive scheme turns to be

$$\tilde{L}(\Theta) = L(\Theta) + \mu \cdot \sum_{i=1}^K \frac{1}{p_i} \quad \text{s.t.} \quad \sum_{i=1}^K p_i = 1. \quad (4)$$

To summarize, we improve the defensive capability of the original DNNs by modifying its loss function as (4), and keep everything else. Of course, due to this modification, the new model should be retrained. That is, the optimal parameters for our defensive network can be obtained by solving

$$\Theta^* = \arg \min_{\Theta} \tilde{L}(\Theta).$$

### 3.3 Analysis of the proposed scheme

Note that the solution of  $\arg \min_{p_k} \sum_{i=1}^K \frac{1}{p_i}$  is  $p_1 = \dots = p_k = \frac{1}{K}$  under the constraints, which indicates that the effect of the regularization term  $\sum_{i=1}^K \frac{1}{p_i}$  is to force  $[p_1, \dots, p_K]^T$  move towards the central point  $[1/K, \dots, 1/K]^T$ . In other words, it will prevent from the point to the positions such as  $[0, \dots, 1, \dots, 0]^T$ . It is natural to worry that this will decrease the classification accuracy of DNNs. In what follows, we claim that this is not the case.

Adding the term  $\sum_{i=1}^K \frac{1}{p_i}$  indeed will cause the minimizer of  $[p_1, \dots, p_K]^T$  move towards  $[1/K, \dots, 1/K]^T$ , but that point will not be reached due to the existence of the first term in the loss function (4). This tendency of moving towards the center part of the simplex is no harm, as what we really care is the correctness of  $i^* = \arg \max_i p_i$ , not the value of  $p_{i^*}$ . Therefore, we do not pursue the large value of  $p_{i^*}$ , as long as  $p_{i^*}$  reaches maximum among all  $p_i$  for  $i = 1, \dots, K$ .

The above argument also reveals a fact that, although it may be different from intuition, high confidence (or over-confidence) on the classification result of one sample is unreliable sometimes. The reason is that over-confidence on one Class  $i$  means that the value of  $p_i$  is large and consequently some values of  $p_j$  should be small for  $j \neq i$ . One extreme case is some  $p_j = 0$  and therefore  $\sum_{i=1}^K \frac{1}{p_K} \rightarrow \infty$ . In other words, this over-confidence sample is sensitive to the adversarial perturbation and therefore vulnerable to adversarial attacks.

The experiments provided in Section 4 will demonstrate that, after using our loss function, the classification accuracy remains while the risk of adversarial phenomenon decreases.

### 3.4 Comparison with Label Smoothing Regularization

Both our scheme and LSR tend to smooth the labels, while the desired label still has the highest probability. To emphasize their difference, we explain LSR and compare these two methods.

The basic procedure of LSR can be described as two steps. Firstly, for  $k \in \{1, \dots, K\}$ , modify the component of one-hot label as:

$$y_k^{LSR} = y_k(1 - \alpha) + \alpha/K,$$

where  $\alpha \in (0, 1)$  is a hyperparameter,  $y_k$  is the label component whose value is 1 for the correct class and 0 for the rest, and  $K$  is the total number of classes. Second, retrain the network with the new labels.

LSR makes the classification clusters much tighter, according to the experiments in [18]. This, to some extent, explains why LSR is effective in adversarial defense. The underlying rationale of LSR, however, is still unknown. LSR needs to have a not commonly accepted prior assumption, i.e., the labels are uniformly distributed for classes other than the true class, while our scheme is based on strict mathematical deduction and does not have such a premise. Therefore, ours has a better explainability.

## 4 Experiments

The main purpose of our experiments is to demonstrate the effectiveness and robustness of our defensive scheme, and therefore to demonstrate the correctness of using the loss function (4).

How to evaluate the capability of a network for defending against adversarial examples is a complicated issue. Here, we illustrate four aspects of the complexities.

1) Adversarial examples is a relative concept. For instance, a sample is an adversarial example for Network  $A$ , it may be a benign sample for Network  $B$ , and vice versa. For instance, the perturbed digits '5' and '6' in Figure 1 are adversarial examples for the network corresponding to Column 2, but not for Column 3.

2) The effect of the perturbation norm. If the norm is sufficiently large, the perturbed image will be significantly different from the original image, therefore it will be "misclassified" as another class. In other words, every sample will be an adversarial example if its perturbation norm is sufficiently large. Therefore, when talking about how to defend against adversarial attack, we usually assume that the perturbation is small. However, the large perturbation norm can be used to show the defensive capability. Given a sample with large perturbation, if it is an adversarial example in Network  $A$  but not in Network  $B$ , we can say that Network  $B$  is "better" for this particular sample.

3) It is not meaningful for talking about defensive capability for a single sample. So some statistical index should be used. Say, given 1000 perturbed images,  $a\%$  of them are misclassified in Network  $A$ , and  $b\%$  of them are misclassified in Network  $B$ . If  $b < a$ , then we can conclude  $B$  is better.

4) Defensive capability depends on different attacking methods. A network, which can defend against perturbed examples generated from the attacking method 1, may fail for the attacking method 2, and vice versa.

Here we design the experiments according to four aspects mentioned above.

For 1), in what follows, our scheme means for a given original network, using the loss function (4) and we have re-trained the network and have obtained its new parameters  $\Theta^*$ . Using the term in the previous description, the original network is  $A$  and our scheme is  $B$ .

For 2), in the case of  $l_2$  norm, we use the perturbation norm defined as  $\varepsilon = \sqrt{\sum_{i=1}^n (x_i - x'_i)^2}$  for two vectors  $\mathbf{x} = [x_1, \dots, x_n]^T$  and  $\mathbf{x}' = [x'_1, \dots, x'_n]^T$ , in which each component is within the interval  $[0, 1]$ .

Note that by our definition,  $\varepsilon = 1$  is a large perturbation. For example, for two vectors from MNIST, if their grey value difference is 10 at each component, then  $\varepsilon = \sqrt{(\frac{10}{255})^2 \cdot 28^2} \approx 1.1$ .

For 3), we use the fooling ratio as the index to show the defensive capability. Its definition is as follows. Given a set of originally correctly classified samples, after adding perturbation, some samples become misclassified. The ratio of the number of misclassified sample to the total sample number is called the fooling ratio. Clearly, the lower the fooling ratio, the better the performance of the network.

For 4), we use ten attacking methods for white-box and black-box attacks, respectively. Most of them have been discussed in Section 2. The white-box attack assumes that the attackers know all the details of the classifier, including the model and parameters, while the black-box attack assumes all the details are unknown and the adversarial examples are fed into the network.

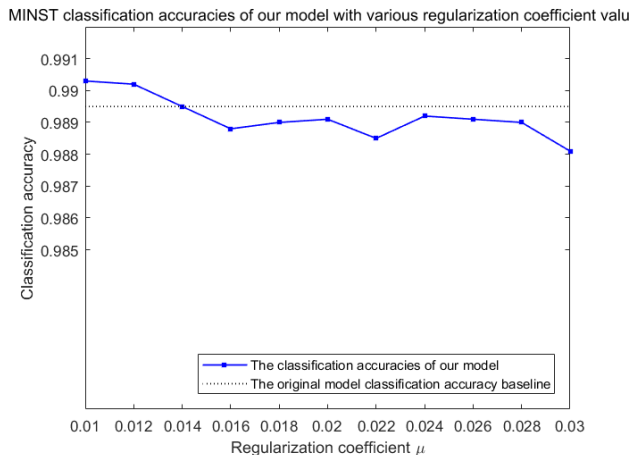


Figure 2: Classification accuracies of the baseline and our scheme with various coefficient values on MNIST under OSSA.

## Datasets and classification methods used in the experiments

In the experiments, three datasets, together with corresponding neural networks, are utilized. These datasets and networks consist of 1) MNIST+ConvNet, 2) CIFAR-10+VGG, and 3) German Traffic Sign Recognition Benchmark (GTSRB)+ResNet. The first two datasets are common benchmarks, and the third one is used as a demonstration for real applications such as autonomous driving.

MNIST [19] is equipped with a simple CNN network, which is a variant of LeNet and called ConvNet here. ConvNet has two convolutional layers with batch normalization and one fully connected layer. Before defensive training, this simple network can reach a classification accuracy of 99%.

CIFAR-10 [20] is equipped with a simplified VGG. This VGG network adopts a variant of simplified 11 layers in order to fit the dataset size. Before defensive training, this model can reach a classification accuracy of around 90.5%.

GTSRB <sup>2</sup> [21] consists of more than 50,000 images of traffic signal in 43 classes. This dataset has 39,209 training images and 12,630 testing images. To facilitate the procedure, we use 39,200 training and 12,600 testing images and rescale the image size to  $32 \times 32$ . GTSRB is equipped with a simplified ResNet with 14 layers to accelerate the training. Before defensive training, the accuracy is around 98.5%.

### 4.1 Defending against white-box attacks

We compare the fooling ratio under 1) various values of the regularization coefficient, 2) various datasets and neural network models, and 3) various attacking methods.

#### Fooling ratios with various values of the regularization coefficient

We compare the capability for generating adversarial examples under various values of the regularization coefficient  $\mu$ , all other parameters are set as the same, i.e., dataset+DNN: MNIST+ConvNet, and the attacking method for generating adversarial examples: OSSA. The purpose of this experiment is to show the effectiveness of our scheme when a suitable value of  $\mu > 0$  is set.

We wish to observe that fooling ratio becomes low, compared with the original network, while the accuracy for the testing data does not decrease using our scheme.

Figures 2 and 3 verify the above claim. Figure 2 shows that, using our scheme, the accuracy remains virtually unchanged, while Figure 3 shows that the fooling ratio significantly decreases.

In Figure 2, the dotted line is the baseline classification accuracy of the original network, i.e., the ConvNet without defensive training, on MNIST. The dotted line is obtained by averaging the accuracies of several experiments. Figure 2 shows that the accuracy remains virtually unchanged (fluctuated around 98.95%) using our scheme.

<sup>2</sup><http://benchmark.ini.rub.de>

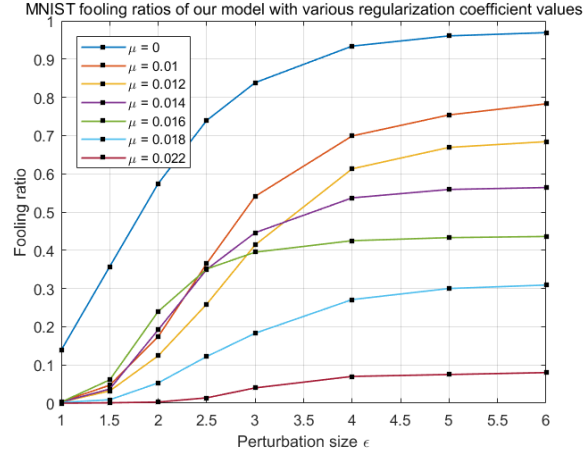


Figure 3: The fooling ratio curves with various regularization coefficient values. All data are obtained on MNIST, using OSSA.

Figure 3 shows that, under certain range of parameters, with the increment of the regularization coefficient  $\mu$ , the fooling ratio of the generated adversarial examples decreases monotonically. When  $\mu = 0.022$  and  $\epsilon = 6$  ( $\epsilon = 6$  is a large distance, as we discussed previously) the fooling ratio is suppressed significantly small (less than 10%), while the classification accuracy is still as high as 98.8% in Figure 2. Since the fooling ratio reflects the defensive capability, low fooling ratio means that the defensive capability is satisfactory.

Figures 2 and 3 demonstrate that our scheme obtains the defensive capability without sacrificing the accuracy.

### Fooling ratios on various datasets and DNNs

In this subsection, we compare the defensive capability for our scheme under various datasets+DNNs, on the same attacking algorithm OSSA. The purpose of this experiment is to evaluate our robustness on different datasets and DNNs.

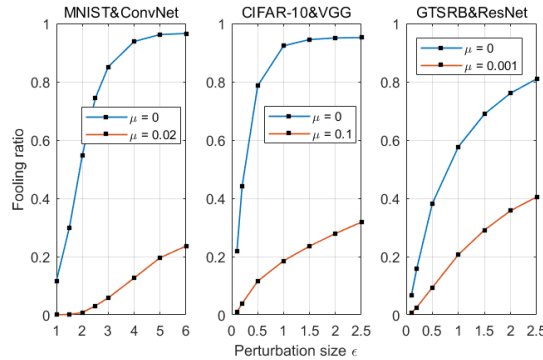


Figure 4: The fooling ratio curves on three datasets with corresponding DNN models, with or without adding  $\mu$ . All experimental data are generated by OSSA.

Figure 4 shows the fooling ratio curves under three datasets and their corresponding DNNs. It reveals that, for all cases, the fooling ratio decreases when a suitable  $\mu > 0$  is set.

### Fooling ratios on various attacking methods

In this subsection, we compare the defensive capability of our scheme under various attacks. The defensive scheme is set as  $\mu = 0.02$  for MNIST+ConvNet. Three non-OSSA one-step attack methods, namely, FGM [9], OTCM [9] and FGSM, are used for the experiment. All three attacking methods are implemented by ourselves. Here OTCM is the acronym for One-step Target Class Method.

The purpose of this experiment is to verify the robustness on various attacking methods.



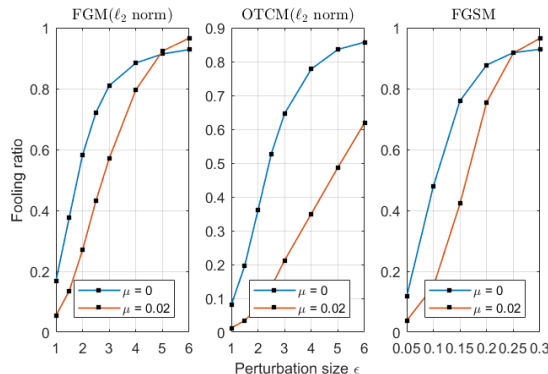


Figure 5: The fooling ratio curves of three adversarial attacking methods on MNIST.

Figure 5 shows that the fooling ratios are low, when the perturbation norm are small (which is the case we are interested in). However, these fooling ratios are high compared with their counterparts in Figure 4. This is reasonable that our method is inspired by [6] where OSSA is proposed. When  $\epsilon$  is large, e.g.,  $\epsilon = 6$ , our scheme fails as the fooling ratio is higher than 60%.

**Defensive capability on more attacking methods using FoolBox** To further evaluate the defensive capability under more attacks, we adopt a toolbox called FoolBox<sup>3</sup> [22] which provides various popular attacking methods.

The toolbox aims to obtain the optimized adversarial examples, i.e., the perturbation should be as small as possible when generating the adversarial examples. So, for a given perturbation norm, it does not generate adversarial examples accordingly. Therefore, we use the distance between the original input and the adversarial example as a measurement for the degree of difficulty for generating an adversarial example in DNNs. The larger the distance, the more difficult the capability of generating adversarial examples, i.e., the better the defensive capability.

Table 1 lists the distances between the original input and the adversarial example, for the original network ( $\mu = 0$ ) and our scheme ( $\mu = 0.024$ ), under nine attacking methods, with MNIST. In the experiments, we load the pretrained model and samples from MNIST as the input for the testing. Then we use the method provided in FoolBox to generate a batch of adversarial examples, and obtain the distance between every adversarial example and its original input. The second column shows the norms used in the attacks. Columns 3 and 4 show the mean distance between the adversarial and original inputs. The above mean distance can be used as a measure for the degree of difficulty on generating adversarial examples, as the same parameters are used for generating adversarial examples for two models. The larger the distance, the more difficult for generating adversarial examples. Table 1 shows that, for all nine methods, our scheme outperforms as our mean distances are larger, and the distance ratio is between 1:1.3 and 1:1.8. This demonstrates the robustness of our method.

Table 1: Comparison of distances between the original input and its adversarial example for two models using MNIST.

Method	Norm	Mean Distance on Original Model	Mean Distance on Our Scheme
FGSM	$l_\infty$	0.107	<b>0.170</b>
FGM	$l_2$	0.00584	<b>0.00791</b>
BIM	$l_1$	0.0210	<b>0.0273</b>
BIM	$l_2$	0.00158	<b>0.00273</b>
BIM	$l_\infty$	0.0726	<b>0.1070</b>
DeepFool	$l_2$	0.00215	<b>0.00267</b>
CW	$l_2$	0.00145	<b>0.00204</b>
JSMA	$l_0$	28.26	<b>48.19</b>
Random PGD	$l_\infty$	0.0730	<b>0.1100</b>

## 4.2 Defending against black-box attacks

Our scheme is further tested for defending against black-box attacks.

<sup>3</sup><https://foolbox.readthedocs.io/en/latest/index.html#>

Table 2 lists the results on MNIST+ConvNet. All adversarial examples are generated by FoolBox, except that OSSA in the last row is generated by ourselves with the parameter  $\varepsilon = 1.0$ . Specifically, given a sample, we use a method provided in the FoolBox and generate an adversarial example for the Network  $A$ . This sample is adversarial for the original network  $A$ , we test whether it is still adversarial for Network  $B$ . Similarly, we can also generate an adversarial example for Network  $B$  and see whether it is adversarial in Network  $A$ . We wish to see, given a batch of samples, using the above operation, samples generated from the original network still have high accuracy (i.e., low fooling ratio) by our scheme, while adversarial examples of our scheme will have a low accuracy for the original network, as we assume our scheme has a higher defensive capability than the original network.

In the table, Columns 2 and 3 show the above cross model classification accuracies. The value (97.47%) in row 1 and column 2 means that, for example, we first use FGSM from FoolBox to attack the original network and generate adversarial examples, and input these adversarial examples to our scheme, then in our scheme the accuracy is 97.47%. This means that the accuracy raises from 0% of the original network to 97.47% of our scheme.

Note that there is no value at the last row and last column. The reason is that our scheme can defend against OSSA significantly and no adversarial examples can be generated for  $\varepsilon = 1.0$ . It seems that the accuracies in column 2 are higher than expected. We analyze the reason as that the adversarial examples generated by FoolBox are optimal with respect to perturbation, which means that it may not be optimal for a defensive model and therefore its defense is relatively easy. In general, the classification accuracy in column 3 is lower than that in column 2, as we have analyzed. Thus we can conclude that our model behaves reasonably acceptable for black-box attacks, although the difference of accuracies is not sufficiently large. It might be combined with other defense techniques to achieve better performance.

Table 2: Cross model classification accuracies on MNIST.

Attacking methods	Generated from original network Tested on our scheme	Generated from our scheme Tested on original network
FGSM ( $l_\infty$ )	97.47%	54.33%
FGM ( $l_2$ )	96.74%	78.18%
BIM ( $l_1$ )	98.79%	93.12%
BIM ( $l_2$ )	98.79%	93.72%
BIM ( $l_\infty$ )	98.89%	89.07%
DeepFool ( $l_2$ )	98.58%	93.64%
CW ( $l_2$ )	98.79%	97.47%
JSMA ( $l_0$ )	96.09%	90.45%
Random PGD ( $l_\infty$ )	98.99%	89.57%
OSSA ( $l_2$ )	92.24%	–

## 5 Conclusion

We have proposed a defensive scheme for adversarial attacks by modifying the loss function of DNNs to control the largest eigenvalue of the FIM. Our scheme stems from the assumption that the vulnerability of DNNs is due to the large value of the largest eigenvalue of FIM. Elaborated by experimental results on typical DNNs with various datasets, our scheme demonstrates its capability of defending against adversarial attacks.

Our contributions can be summarized as: 1) Our scheme is a simple yet effective regularization method. Compared with other adversarial training methods, it only needs to retrain once; 2) our scheme has an explainable property compared with LSR; and 3) the effectiveness is demonstrated by various DNNs on common datasets.

Future work can be focused on using the theory of simplex to further improve the loss function, as the density vectors are on a simplex.

## References

- [1] C. Szegedy, W. Zaremba, I. Sutskever, J. Bruna, D. Erhan, I. Goodfellow, and R. Fergus, “Intriguing properties of neural networks,” *ArXiv preprint, arXiv:1312.6199*, 2013.
- [2] B. Biggio, I. Corona, D. Maiorca, B. Nelson, N. Srndic, P. Laskov, G. Giacinto, and F. Roli, “Evasion attacks against machine learning at test time,” in *Joint European Conference on Machine Learning and Knowledge Discovery in Databases*, 2013, pp. 387–402.

- [3] Y. Vorobeychik and M. Kantarcioglu, *Adversarial Machine Learning*, Morgan & Claypool Publishers, 2018.
- [4] I. Goodfellow, J. Shlens, and C. Szegedy, “Explaining and harnessing adversarial examples,” in *International Conference on Learning Representations*, 2015.
- [5] S. M. Moosavidezfooli, A. Fawzi, O. Fawzi, P. Frossard, and S. Soatto, “Analysis of universal adversarial perturbations,” *ArXiv preprint, arXiv:1705.09554*, 2017.
- [6] C. Zhao, T. Fletcher, M. Yu, Y. Peng, G. Zhang, and C. Shen, “The adversarial attack and detection under the Fisher information metric,” in *Proceedings of the thirty-third AAAI Conference on Artificial Intelligence*, 2019, pp. 5869–5876.
- [7] C. Szegedy, V. Vanhoucke, S. Ioffe, J. Shlens, and Z. Wojna, “Rethinking the inception architecture for computer vision,” in *Proceedings of the IEEE Conference on Computer Vision and Pattern Recognition*, 2016, pp. 2818–2826.
- [8] A. Kurakin, I. Goodfellow, and S. Bengio, “Adversarial examples in the physical world,” *ArXiv preprint, arXiv:1607.02533*, 2016.
- [9] A. Kurakin, I. Goodfellow, and S. Bengio, “Adversarial machine learning at scale,” *ArXiv preprint, arXiv:1611.01236*, 2016.
- [10] N. Carlini and D. A. Wagner, “Towards evaluating the robustness of neural networks,” in *IEEE Symposium on Security and Privacy*, 2017, pp. 39–57.
- [11] S. M. Moosavidezfooli, A. Fawzi, and P. Frossard, “Deepfool: A simple and accurate method to fool deep neural networks,” in *IEEE Conference on Computer Vision and Pattern Recognition*, 2016, pp. 2574–2582.
- [12] N. Papernot, P. McDaniel, S. Jha, M. Fredrikson, Z. B. Celik, and A. Swam, “The limitations of deep learning in adversarial settings,” in *IEEE European Symposium on Security and Privacy*, 2016, pp. 372–387.
- [13] A. Madry, A. Makelov, L. Schmidt, D. Tsipras, and A. Vladu, “Towards deep learning models resistant to adversarial attacks,” in *International Conference on Learning Representations*, 2018.
- [14] J. M. Danskin, *The Theory of Max-Min and its Application to Weapons Allocation Problems*, Springer, Berlin, 1967.
- [15] J. Buckman, A. Roy, C. Raffel, and I. Goodfellow, “Thermometer encoding: One hot way to resist adversarial examples,” in *International Conference on Learning Representations*, 2018.
- [16] D. Warde-Farley and I. Goodfellow, “Adversarial perturbations of deep neural networks,” in *Perturbations, Optimization, and Statistics*, p. 311. 2016.
- [17] M. Goibert and E. Dohmatob, “Adversarial robustness via adversarial label-smoothing,” *ArXiv preprint, arXiv:1906.11567*, 2019.
- [18] R. Müller, S. Kornblith, and G. Hinton, “When does label smoothing help?,” *ArXiv preprint, arXiv: 1906.02629.*, 2019.
- [19] Y. LeCun, C. Cortes, and C. J.C. Burges, “MNIST handwritten digit database,” Tech. Rep., 1998.
- [20] A. Krizhevsky, “Learning multiple layers of features from tiny images,” Tech. Rep., University of Toronto, 2009.
- [21] J. Stallkamp, M. Schlipsing, J. Salmen, and C. Igel, “Man vs. computer: Benchmarking machine learning algorithms for traffic sign recognition,” *Neural Networks*, vol. 32, pp. 323–332, 2012.
- [22] J. Rauber, W. Brendel, and M. Bethge, “Foolbox v0.8.0: A Python toolbox to benchmark the robustness of machine learning models,” Tech. Rep., 2017.